Prototyping airborne ultrasonic arrays

Asier Marzo

Abstract Focused ultrasound is the base mechanism for mid-air tactile feedback generation, acoustic levitation, wireless power transfer, directional audio and other emerging applications. The basic required setup is an ultrasonic emitter with the capability of focusing its acoustic power at a target point. Ideally, a multi-emitter phased array is used since it is capable of steering and shaping the sound field with millimetre accuracy and a time response in the order of milliseconds. There are compelling commercial products and open designs for this kind of ultrasonic arrays. Here, we review the different elements that compose an ultrasonic array: from the emitters and the driving electronics to the signal generators or algorithms. We review some techniques to simulate the output of ultrasonic arrays or to determine the emission phases for target fields. Also, we provide some suggestions for future challenges related to cost, power, and heat reduction.

1 Introduction

Transmitting phased arrays are devices made of multiple emitters that can adjust the phase (i.e. time delay) and amplitude of each element in order to focus their power at specific points or directions. This focusing and steering can be done electronically, at fast speeds and with high-accuracy without the need of mechanically moving the array. Phased-arrays are nowadays used in 5G communications [1] but have been commonly used in radar [2], sonar [3] and medical ultrasound [4]. When the arrays are composed of airborne ultrasonic emitters, it is possible to focus the acoustic amplitude at different points in space; by applying a modulation on the emitted wave, these points can be perceived as tactile stimuli by the mechanoreceptors of the human hand [5, 6, 7, 8].

Asier Marzo
UpnaLab, Institute of Smart Cities, Public University of Navarre, Spain. e-mail: asier.marzo@unavarra.es

Airborne ultrasonic phased-arrays (AUPs) can also be used for acoustic levitation [9, 10], wireless power transfer [11] or the generation of directional audio beams [12, 13]. The AUPs can be dynamically focused, this enables to move the particles in levitation, transfer power only to specific receivers in wireless power, and deliver sound to moving people in directional audio. An AUP can be used in conjunction with virtual reality systems [14] to generate the missing tactile sensations when touching virtual objects without forcing the user to wear devices on their hands. Other use cases can be found in hands-free car interfaces [15] or kiosks with gestural input [16].

This chapter focuses on describing the main elements that form an AUP. The main ones are the ultrasonic emitters, the amplification drivers, and the signal generators. Some of these elements are commercially available. We will also see common spatial arrangement of the emitters used for the AUP. The chapter finishes with a review on the main simulation techniques and algorithms.

2 Components

A phased array has 3 main components. Firstly, the ultrasonic elements that transduce the electrical signal into ultrasonic waves. Since we focus on emission arrays, also called transmission arrays, we use ultrasonic emitters, but other types of arrays have elements that receive (receivers) or that perform both functions (transducers). Secondly, the driver electronics that amplify the logic signal into a signal capable of driving the emitters with enough amplitude; in general, emitters based on piezoelectric transduction have high impedance, require high-voltage and low-current. Thirdly, the signal generators capable of producing multiple synchronised signals of adjustable phase and amplitude.

2.1 Emitters

The main commercially available ultrasonic emitters used in phased-arrays have 1 cm in diameter, larger emitters are available but 1 cm is closer to the operating wavelength (8.46mm) and thus can create more accurate fields and focal points. These emitters are based on leaky-plate radiation and operate at 40 kHz; some common models are MA40S4S (Murata Electronics, Japan), MSO-P1040H07T (Manorshi, China) or FBULS1007P-T (Ningbo, China). Inside these emitters, there is a thin piezoelectric disk that vibrates in radial mode, the disk is attached to a metal plate so that the radial vibration is transformed into traversal vibration, a metal cone is attached on top of this metal plate and allows to radiate from the metal plate into air despite the large mismatch of acoustic impedance. Variations of these transducers can be found with different diameters (e.g. 1.6 cm) or materials for the casing (plastic or aluminium) Fig. 1.a. The cone is exposed directly at the top but protected with a

metal grid or a plastic pattern that also helps to tune the directivity pattern. These emitters are mainly available at 40 kHz, but it is also possible to find them operating at 25 kHz or 58 kHz.

In the supplementary information of [17], a table with radiation amplitude and aperture can be found for different ultrasonic emitters. These parameters can be used in the equations presented in section 4 to obtain an estimation of the field at different points around the emitters. In general, the emitters are driven with a square wave signal [18] leading to simpler driving electronics and generation with digital components. Excitation signals of 24 Vpp are normal in continuous operation, with the metal-case emitters being able to take up to 50 Vpp continuously. The current consumption varies from 4 to 10 mA depending on the efficiency of the driving electronics. Some ultrasonic emitters are made of a piezoelectric elements directly bonded to a metal case. These transducers are water-proof, robust and easy to cool down (e.g. MCUST18A40B12RS, Multicomp). However, their radiation into air is not as effective as the previously described leaky-plate emitters since closed-case emitters are designed to be bonded into a solid material, for example in distance measure applications in small boats [19].

There are wideband ultrasonic emitters made of a piezo-element attached to a plastic membrane. These emitters are generally sold as pest control technology (e.g. FBUT3813, NingBo). They are less efficient than the previous models but can emit with a wide range of frequencies. In the same spectrum, compression drivers (Fig. 2.c) [20] have often been used as ultrasonic emitters for levitation experiments and perhaps could be used for haptic applications.

Commercially available transducers of frequencies larger than 100 kHz are available, they employ a different working principle. The base is a metal case with a piezo attached on the front face from the inside. To provide correct transmission from the case into air, a white porous material is used as the matching layer. These transducers are available operating at 100, 200, and 400 kHz (Fig. 2.b). However, they have a diameter of dozens of wavelengths, therefore having little capability to create wave interferences and be used in phased-arrays.

Custom-made emitters can be found in the research literature. For example, large bulks of metal clamping piezo electric elements are called Langevin transducers

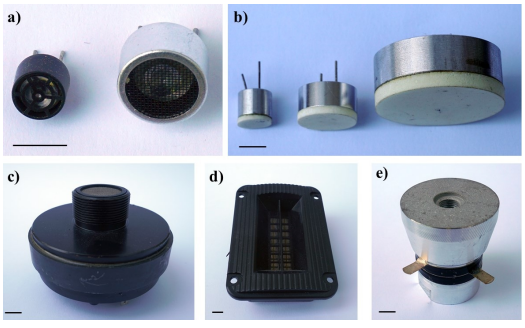

Fig. 1 Different ultrasonic emitters. The black lines at the bottom left of each Figure are for reference. They are all 10 mm. a) Leaky-plate open case operating at 40 kHz of diameter 10 mm and 16 mm. b) High-frequency transducers with porous matching layer operating at 400, 200, and 100 kHz. c) Compression drive. d) Membrane based tweeter. e) Langevin horn.

(Fig. 2.d) and are widely used for high-intensity ultrasound applications [21, 22]. However, their use in phased arrays would not be feasible since it is difficult to manufacture them in a small size (they are more than 3 or 4 times the wavelength). More importantly, it is hard to build them with similar resonant frequencies; to obtain two emitters with similar frequencies, the method was to build a dozen of horns and select the closest pair [21]. Also, these Langevin horns are quite sensitive to continuous emission due to changes in temperature and the required voltage to drive them is dangerous (>200 V). Consequently, some airborne ultrasonic systems are moving from Langevin-based emitters to commercially available leaky-plate transducers [23].

Some research groups have created wideband high-frequency transducers [24] but no arrays for haptic feedback have been realized yet. Flexible transducers made of PVDF are also a promising technology [25] but still not suitable for a full phased-array due to their low-power, and even less for prototyping AUPs.

2.2 Drivers

The signal coming from the signal generators usually does not have enough amplitude for exciting the emitters with sufficient power. Most of the times, the ultrasonic emitters are the most expensive parts of the arrays and thus. For this reason, they should be driven at their maximum voltage, so as to achieve as much acoustic amplitude as possible with the minimum number of emitters.

If a sinusoidal signal is used, then audio amplifiers [26] or even RF amplifiers [27] can be used to amplify the analog signal. However, most of the AUPs use square waves, which are usually amplified with Mosfet drivers [18]. Mosfet drivers are a good option since they are designed to drive the highly capacitive gates of Mosfets; there are several theoretical models to describe an ultrasonic piezoelectric emitter and how their main load is of capacitive nature [28].

The drivers can operate in push mode, in which one terminal of the emitter is connected to ground (or voltage) and the other terminal connects to the oscillating signal of the driver [29]. Another possibility is to drive the emitter in push-pull mode, where both legs connect to two signals that are out of phase [17]; thereby, the voltage peak-to-peak that is applied into the emitter is double of the supplied voltage, although two driver channels are needed per emitter in this case.

Most ultrasonic emitters present a high-impedance (e.g. 1 kOhm) when compared to traditional speakers, therefore most drivers are not designed to drive them efficiently. Electrical matching can be done with different circuit networks [30] or with a matching transformer [31] that also increases the voltage delivered to the emitters.

2.3 Signal generation

Using an off-the-shelf signal generator can be feasible for generating 1 or 2 channels. Depending on the requirements for the signal, a scientific instrument (e.g. Keysight Technologies 33210A in the order of EUR 1000) or just a breakout board based on a direct digital synthesis IC (e.g. AD9851 Analog Devices at EUR 15) will suffice. For focusing, a phase resolution of 5 divisions per period leads to optimum amplitudes at the focal point, since increasing the phase resolution further only improves the amplitude by 5% [18]. For more complex amplitude patterns, like the ones shown in Sec. 5.3, a phase resolution of 8 divisions per period produces the optimum results, as adding further phase resolution only decreases the Mean Square Error by 3% [29]. Steering the beam at specific angles will require more phase resolution, especially if the beam needs target points at long distances from the array. For haptic AUPs, steering with high accuracy is not as important as focusing at different point around the array since the user's hand is not further than 1 m. The low requirements on phase resolution but the necessity of a high number of channels leads to the use of other signal generators in AUPs for haptic.

The traditional 555 IC is used in some projects when only one channel is required; however, it is not possible to synchronize multiple of them. An Arduino UNO can generate at least 2 channels with phase control [17] and an Arduino MEGA, up to 64 channels with 10 divisions per period [18]. However, when more channels or phase control are needed, a solution based on an FPGA is commonly employed [32, 29]. Hybrid architectures like the BeagleBone [33] have been successfully used and new microcontrollers like the ESP32 or Raspberry Pi Pico are promising alternative still to be tested since they include protocols for parallel output of data at controlled speeds.

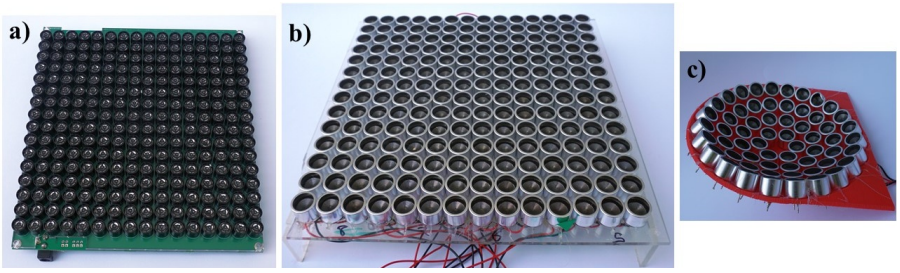

Fig. 2 Basic array geometries. a) a 16x16 flat array made with 10 mm diameter emitters. b) a 16x16 flat array using 16 mm emitters. c) a bowl of radius of 100 mm made with 60 emitters of 16 mm diameter.

3 Geometries

The location of the ultrasonic emitters determines the main capabilities of the arrays such as the amplitude that can be obtained at the focal points, the dimensions of those points, the undesired secondary lobes that appear and the working volume in which the array can be focused effectively.

A flat geometry is used in most commercial products, since it allows for soldering the emitters directly in a PCB and thus enable easy manufacturing. The rectangular distribution is the simplest because it is panelizable and it does not leave gaps (Fig. 2). A more efficient geometry is the hexagonal packing, which gives more density of emitters but leaves gaps and makes it harder to put components on the other side of the array or to tile various arrays. Arrays with uniform distribution of emitters lead to the generation of undesired focal points (side lobes) that appear outside the main target focal point. To avoid this problem, distributions with quasi-random [34] or Fibonacci arrangements [35] have shown to reduce sidelobes; however, their manufacturing in a PCB is more complicated.

Emitters do not need to be constrained to a flat surface if extension wires are used to decouple their driving electronics. Spherical caps (Fig. 2.c) generate focal points with more amplitude [17], however the working volume in which they can be focused gets reduced. In other words, flat arrays can focus on a larger volume but with less power. Furthermore, spherical caps have a natural focus which can be used to remove the necessity for complex electronics if only a static focal point is desired. That is, when all the emitters are driven with the same signal a focal point is generated at the geometric focus.

Height offset on the emitters can be used to produce phase changes at a point without the need of using different electrical signals [36], this technique has been used to generate vortices [37], twin-traps or other acoustic fields by placing the emitters at specific positions. This reduces the complexity on the electronics but the arrays does not have the capability to focus at different points. Passive phase modulators can also be used for focusing and shaping the acoustic field emitted from AUPs [36, 38, 39].

Using multiple arrays or extended ones is a technique used to cover a larger working volume [40] or being able to focus at different positions around a 3d object [41, 42]. Please refer to chapter X. Other types of spatial distributions such as V-shape or ring shape have been presented in the literature (See supplementary information of [43]), but they are not commonly used for haptic arrays.

4 Simulation of the emitted field

The piston model is an simplification commonly used to calculate the incident field generated by one or multiple emitters [44]. The model is only applicable for the far-field of the emitters, but this is not an issue since most tactile stimulation takes place centimetres away from the array, the far-field of the employed ultrasonic emitters

starts at 3 mm approximately from their top. The near to far-field limit starts at $(2a)^2/4\lambda$, where λ is the wavelength and a is the emitter radius [45]. The piston model cannot be used for simulating domains with complex reflecting geometry but this is usually not a problem because tactile systems radiate directly onto the user's hand. Reflections on planar objects can be approximated by mirroring the emitters and adding an attenuation coefficient depending on the material of the reflector. This method is fast and can run in real time for hundreds of emitters [18].

The complex acoustic pressure $p(\boldsymbol{r})$ at point $\boldsymbol{r}$ due to a piston source emitting at a single frequency can be modelled as:

$$p(\boldsymbol{r}) = AV\frac{D_f(\theta)}{d}e^{i(\varphi+kd)} \tag{1}$$

Where A is the transducer output efficiency and V is the excitation signal peak-to-peak amplitude. The term $\frac{1}{d}$ is the divergence, where d is the distance between the center of the piston and the point $\boldsymbol{r}$. $k = 2\pi/\lambda$ is the wavenumber and λ is the wavelength. φ is the emitting phase of the source. D_f is the directivity function of the emitter and depends on the angle θ between the emitter normal and the point $\boldsymbol{r}$. The directivity function of a vibrating piston source can be expressed as:

$$D_f = 2J_1(ka\sin\theta)/ka\sin\theta \tag{2}$$

Where J_1 is a first order Bessel function of the first kind and a is the radius of the piston. This directivity function can be approximated as $D_f = \mathrm{sinc}(ka\sin\theta)$.

The total acoustic field P generated by N transducers is the addition of their emitted complex fields, i.e. $P = \sum_{j=1}^{N} p_j$. The constant A and the piston radius a are needed to characterize a transducer. For instance, the commonly used MA40S4S (Murata Electronics, Japan) can be approximated as: a=4.5 mm and A=0.17 $Pa{\cdot}m/V$.

This simple model can be used to simulate the shape and amplitude of the focal points generated by different array geometries. For instance, in Fig. 3, we compare a flat 16×16 array made with 10 mm emitters (MA40S4S) and 16 mm emitters (MSO-P1040H07T). It can be seen that the 16 mm emitters produce a stronger and smaller focal point around a larger working volume but sidelobes are closer to the main focal point. Also, an array made with 16 mm emitters is larger and more cumbersome.

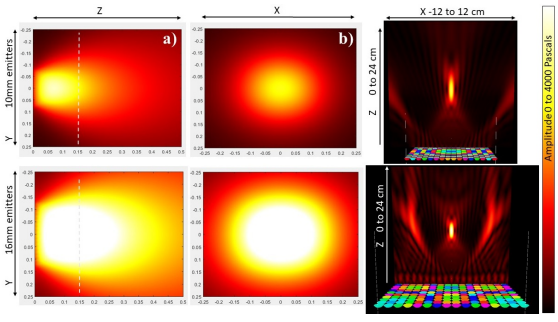

Fig. 3 Amplitude at the focal point when the arrays are focused at each point of the slice. 16×16 flat arrays made of Murata MA40S4S 10mm emitters (top row) and 16 mm Manorhsi MSO-P1040H07T emitters (bottom row) are compared. On the third column, the shape of a focal point is shown.

5 Focusing algorithms

Multiple techniques have been developed to determine the required emission phases of each emitter so that the array focuses the acoustic power at different positions. We divide them in 3 categories: single focal point, multiple focal points, and the generation of a 2D amplitude pattern (also called acoustic image).

5.1 Simple focus

To focus the acoustic power at a position in space, the incoming wave from each emitter should arrive at that point with the same phase. This leads to a simple time of flight algorithm $\varphi_n = k\,|f - s_n|$, where φ_n is the emission phase for the n emitter, f is the position of the target focal point, s_n is the position of transducer n, and $|\cdot|$ the distance between those two points. Also please refer to chapters 1 and 14. Apodization techniques, such as applying a Gaussian profile on the amplitude of the emitters, can be used to reduce the sidelobes [46] or give a rounder profile to the focal point.

5.2 Multi-focus

There are 3 main techniques for creating multiple focal points at target positions. In the first one [47, 48], the emitters are split into different groups using a checkboard pattern or other type of spatial division, each subset of emitters is focused with the simple focus method at a position. This method is fast to compute, leads to smooth transitions, but it does not provide optimum results in terms of amplitude, since the emitters may interfere between subsets.

The creation of multiple focal points can be set as an optimization problem with the emission phases as the variables, and the addition of the amplitude at the target

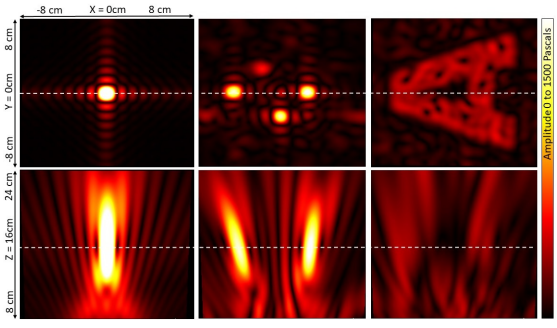

Fig. 4 Amplitude field resulting from focusing a phased array using different algorithms. The array has 16x16 1cm emitters (Murata MA40S4S), the slices are taken 16cm above the array. a) single focal point. b) three focal points. c) amplitude target of a letter A.

points as the target function. Optimizations solved by mean root squares [5, 49] or Broyden–Fletcher–Goldfarb–Shanno (BFGS) [43] have been used with success.

Iterative back propagation (IBP) [50] can also be used to find emission phases that create maximum amplitude at the target points. Variations of this method such as GS-SPAT [51] lead to fast calculations that allow the movement of the focal points at high speeds (in excess of 10 kHz). For details, please refer to chapter XI.

5.3 Amplitude images

For some applications, it is desired to project an amplitude pattern that resembles that of an image, it could be a simple shape such as a circle or a more complex one like a dove. However, for haptic applications, simple shapes are enough since complex shapes cannot be discerned correctly by humans. Holograms for acoustics [52] is an emergent field with the aim of modulating acoustic waves into target amplitude fields, normally a passive phase modulator of high spatial resolution is employed, but algorithms adapted to phased-arrays are also present in the literature [29].

6 Conclusion

We have presented the main components that form an ultrasonic airborne phased-array used for mid-air haptic stimulation. We have analysed the main types of commercially-available ultrasonic emitters, driver electronics and signal generators. We showed some of the common geometries for the spatial disposition of the emitters. Algorithms and simulation methods for phased-arrays were briefly introduced. There are multiple companies that commercialize phased-arrays, also it is still possible to build arrays at home and customise them in shape or power. This fosters novel applications and a growing community of both researchers and enthusiasts that will experiment with phased array for mid-air haptic feedback.

Acknowledgements This research was funded by Jovenes Investigadores Grant (UPNA, Spain) and from the European Union's Horizon 2020 research and innovation programme under grant agreement No 101017746, TOUCHLESS.

References

1. R. Flamini, C. Mazzucco, R. Lombardi, C. Massagrande, F. Morgia, A. Milani, in *2019 IEEE International Symposium on Phased Array System & Technology (PAST)* (IEEE, 2019), pp. 1–2
2. A.J. Fenn, D.H. Temme, W.P. Delaney, W.E. Courtney, Lincoln Laboratory Journal **12**(2), 321 (2000)

3. A. Baggeroer, in *AIP Conference Proceedings*, vol. 760 (American Institute of Physics, 2005), vol. 760, pp. 3–24
4. R. Seip, W. Chen, J. Tavakkoli, L. Frizzell, N. Sanghvi, in *Proc. 3rd Int. Symp. Therapeutic Ultrasound* (2003), pp. 423–428
5. L.R. Gavrilov, Acoustical Physics **54**(2), 269 (2008)
6. T. Carter, S.A. Seah, B. Long, B. Drinkwater, S. Subramanian, in *Proceedings of the 26th annual ACM symposium on User interface software and technology* (2013), pp. 505–514
7. T. Hoshi, T. Iwamoto, H. Shinoda, in *World Haptics 2009-Third Joint EuroHaptics conference and Symposium on Haptic Interfaces for Virtual Environment and Teleoperator Systems* (IEEE, 2009), pp. 256–260
8. I. Rakkolainen, A. Sand, R. Raisamo, in *2019 IEEE International Symposium on Multimedia (ISM)* (IEEE, 2019), pp. 94–944
9. Y. Ochiai, T. Hoshi, J. Rekimoto, ACM Transactions on Graphics (TOG) **33**(4), 1 (2014)
10. M.A. Andrade, A. Marzo, J.C. Adamowski, Applied Physics Letters **116**(25), 250501 (2020)
11. R. Morales González, A. Marzo, E. Freeman, W. Frier, O. Georgiou, in *Proceedings of the Fifteenth International Conference on Tangible, Embedded, and Embodied Interaction* (2021), pp. 1–13
12. Y. Ochiai, T. Hoshi, I. Suzuki, in *Proceedings of the 2017 CHI Conference on Human Factors in Computing Systems* (2017), pp. 4314–4325
13. A.C. Bourland, P. Gorman, J. McIntosh, A. Marzo, Interactions **25**(5), 16 (2018)
14. O. Georgiou, C. Jeffrey, Z. Chen, B.X. Tong, S.H. Chan, B. Yang, A. Harwood, T. Carter, in *2018 IEEE Conference on Virtual Reality and 3D User Interfaces (VR)* (IEEE, 2018), pp. 553–554
15. O. Georgiou, V. Biscione, A. Harwood, D. Griffiths, M. Giordano, B. Long, T. Carter, in *Proceedings of the 9th International Conference on Automotive User Interfaces and Interactive Vehicular Applications Adjunct* (2017), pp. 233–238
16. J.R. Kim, S. Chan, X. Huang, K. Ng, L.P. Fu, C. Zhao, in *Extended Abstracts of the 2019 CHI Conference on Human Factors in Computing Systems* (2019), pp. 1–4
17. A. Marzo, A. Barnes, B.W. Drinkwater, Review of Scientific Instruments **88**(8), 085105 (2017)
18. A. Marzo, T. Corkett, B.W. Drinkwater, IEEE transactions on ultrasonics, ferroelectrics, and frequency control **65**(1), 102 (2017)
19. F. Giordano, G. Mattei, C. Parente, F. Peluso, R. Santamaria, Sensors **16**(1), 41 (2016)
20. N. Ramachandran, *Modeling and control of acoustic levitation for dust control application* (Southern Illinois University at Carbondale, 2010)
21. J. Weber, C. Rey, J. Neuefeind, C. Benmore, Review of scientific instruments **80**(8), 083904 (2009)
22. D. Foresti, M. Nabavi, M. Klingauf, A. Ferrari, D. Poulikakos, Proceedings of the National Academy of Sciences **110**(31), 12549 (2013)
23. R.H. Morris, E.R. Dye, P. Docker, M.I. Newton, Physics of Fluids **31**(10), 101301 (2019)
24. J. Topete, T.G. Alvarez-Arenas, in *SENSORS, 2014 IEEE* (IEEE, 2014), pp. 102–105
25. L.F. Brown, J.L. Mason, IEEE transactions on ultrasonics, ferroelectrics, and frequency control **43**(4), 560 (1996)
26. R.S. Schappe, C. Barbosa, The Physics Teacher **55**(1), 6 (2017)
27. A. Franklin, A. Marzo, R. Malkin, B. Drinkwater, Applied Physics Letters **111**(9), 094101 (2017)
28. Introduction to ultrasonic drivers (2019). URL https://www.piezodrive.com/ultrasonic-drivers/intro-ultrasonic/
29. R. Morales, I. Ezcurdia, J. Irisarri, M.A. Andrade, A. Marzo, Applied Sciences **11**(7), 2981 (2021)
30. V.T. Rathod, Electronics **8**(2), 169 (2019)
31. L. Svilainis, G. Motiejūnas, Ultragarsas/Ultrasound **58**(1), 30 (2006)
32. S. Zehnter, C. Ament, in *2019 IEEE International Ultrasonics Symposium (IUS)* (IEEE, 2019), pp. 654–658
33. Open source ultrasonic phased array. URL https://hackaday.io/project/159467-open-source-ultrasonic-phased-array

34. P.B. Rosnitskiy, B.A. Vysokanov, L.R. Gavrilov, O.A. Sapozhnikov, V.A. Khokhlova, IEEE transactions on ultrasonics, ferroelectrics, and frequency control **65**(4), 630 (2018)
35. A. Price, B. Long, in *2018 IEEE International Ultrasonics Symposium (IUS)* (IEEE, 2018), pp. 1–4
36. A. Marzo, A. Ghobrial, L. Cox, M. Caleap, A. Croxford, B. Drinkwater, Applied Physics Letters **110**(1), 014102 (2017)
37. Ultrasonic screwdriver in air - angular momentum transfer to matter (2015). URL https://www.youtube.com/watch?v=vqe3YvhivYU
38. G. Memoli, M. Caleap, M. Asakawa, D.R. Sahoo, B.W. Drinkwater, S. Subramanian, Nature communications **8**(1), 1 (2017)
39. M.A. Norasikin, D. Martinez Plasencia, S. Polychronopoulos, G. Memoli, Y. Tokuda, S. Subramanian, in *Proceedings of the 31st Annual ACM Symposium on User Interface Software and Technology* (2018), pp. 247–259
40. B. O'Conaill, J. Provan, J. Schubel, D. Hajas, M. Obrist, L. Corenthy, in *Extended Abstracts of the 2020 CHI Conference on Human Factors in Computing Systems* (2020), pp. 1–8
41. T. Ohmori, Y. Abe, M. Fujiwara, Y. Makino, H. Shinoda, in *Extended Abstracts of the 2021 CHI Conference on Human Factors in Computing Systems* (2021), pp. 1–5
42. T. Ohmori, Y. Abe, M. Fujiwara, Y. Makino, H. Shinoda, *Remote Friction Control on 3-Dimensional Object Made of Polystyrene Foam Using Airborne Ultrasound Focus* (Association for Computing Machinery, New York, NY, USA, 2021). URL https://doi.org/10.1145/3411763.3451598
43. A. Marzo, S.A. Seah, B.W. Drinkwater, D.R. Sahoo, B. Long, S. Subramanian, Nature communications **6**(1), 1 (2015)
44. H. O'Neil, The Journal of the Acoustical Society of America **21**(5), 516 (1949)
45. T. Lilliehorn, U. Simu, M. Nilsson, M. Almqvist, T. Stepinski, T. Laurell, J. Nilsson, S. Johansson, Ultrasonics **43**(5), 293 (2005)
46. J. Guo, L. Chen, Y. Zhang, K. Yang, J. Li, X. Gao, in *2013 Far East Forum on Nondestructive Evaluation/Testing: New Technology and Application* (IEEE, 2013), pp. 181–188
47. M.A. Andrade, T.S. Camargo, A. Marzo, Review of Scientific Instruments **89**(12), 125105 (2018)
48. A. Watanabe, K. Hasegawa, Y. Abe, Scientific reports **8**(1), 1 (2018)
49. B. Long, S.A. Seah, T. Carter, S. Subramanian, ACM Transactions on Graphics (TOG) **33**(6), 1 (2014)
50. A. Marzo, B.W. Drinkwater, Proceedings of the National Academy of Sciences **116**(1), 84 (2019)
51. D.M. Plasencia, R. Hirayama, R. Montano-Murillo, S. Subramanian, ACM Transactions on Graphics (TOG) **39**(4), 138 (2020)
52. K. Melde, A.G. Mark, T. Qiu, P. Fischer, Nature **537**(7621), 518 (2016)